Supporting Information

Designing Hybrid Chiral Photonic Films with Circularly Polarized Room-Temperature Phosphorescence

Mingcong Xu,[†] Xueyun Wu,[†] Yang Yang,[‡] Chunhui Ma,[†] Wei Li,[*,†] Haipeng Yu,[†] Zhijun Chen,[†] Jian Li,[†] Kai Zhang,[*,‡] and Shouxin Liu[*,†]

[†]Key laboratory of Bio-based Material Science and Technology of Ministry of Education, Northeast Forestry University, Harbin 150040, China,

[‡]Wood Technology and Wood Chemistry, Dept. Wood Technology and Wood-based Composites, University of Goettingen, Büsgenweg 4, 37077 Göttingen, Germany

* E-mail: liwei19820927@126.com; kai.zhang@uni-goettingen.de; liushouxin@126.com

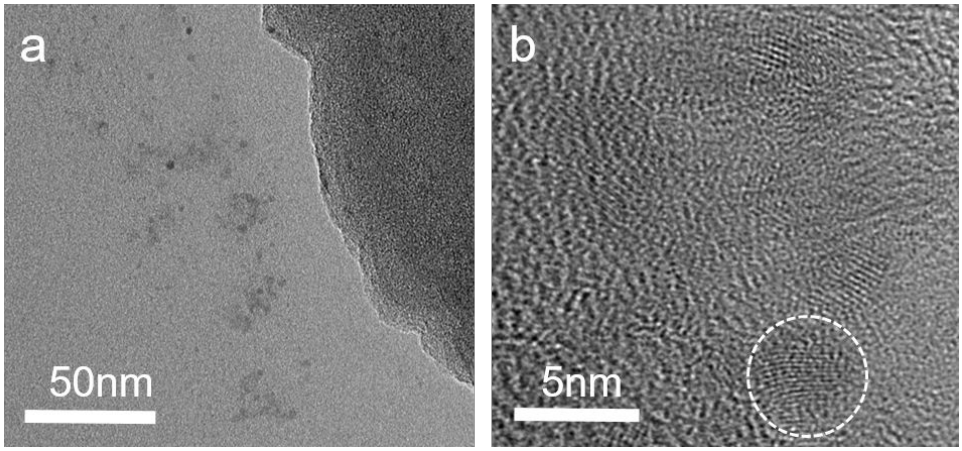

Figure S1. (a) Representative TEM image of carbon dots (CDs). (b) High-resolution (HR) TEM image of CDs.

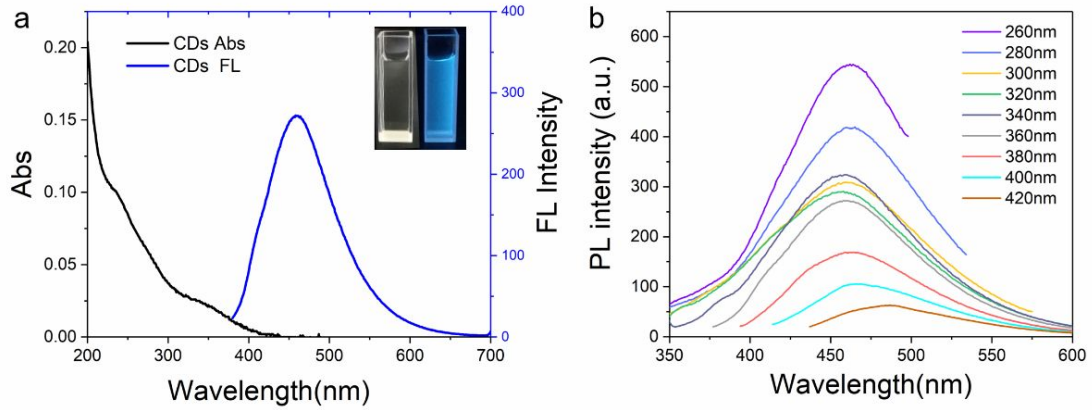

Figure S2. (a) UV-vis absorption spectra and FL emission spectra of the CDs dispersion. Inset is the photograph of the CDs dispersion taken under natural light (left) and 365 nm UV light (right). (b) FL emission spectra of the CDs dispersion excited at various wavelengths.

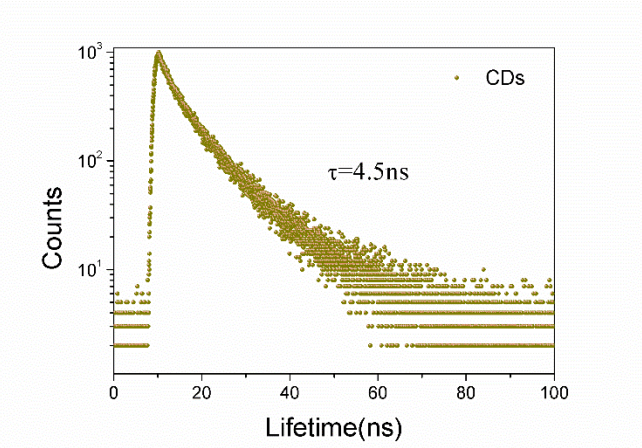

Figure S3. Time-resolved photoluminescence decay curves of CDs solution.

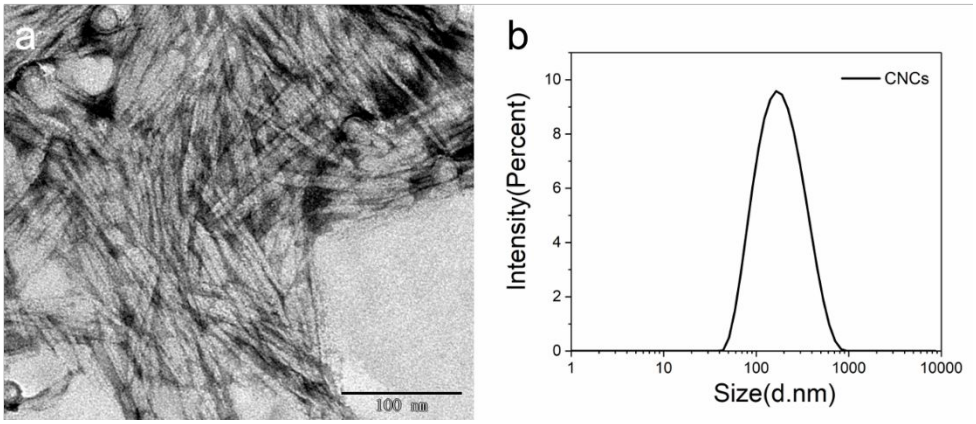

Figure S4. (a) Representative TEM image of cellulose nanocrystals (CNCs). (b) dynamic light scattering (DLS) curve of CNCs.

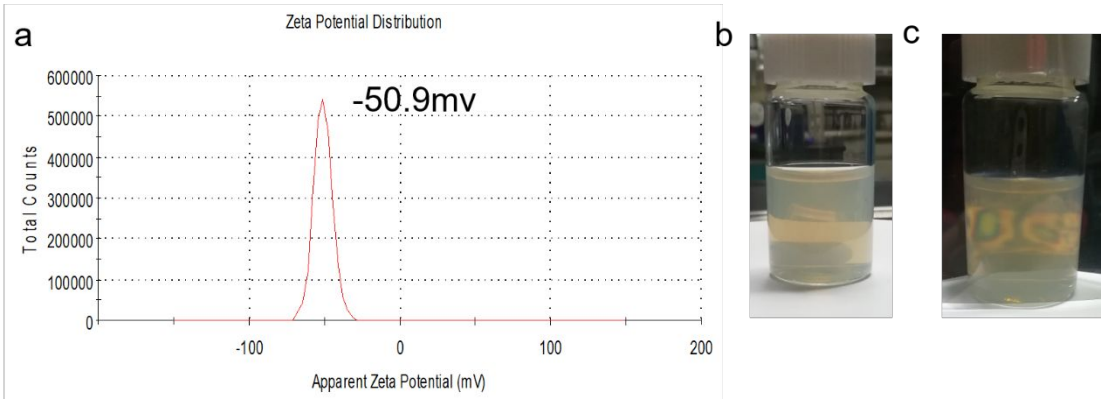

Figure S5. (a) Zeta potential measurement of CNCs. (b) Photograph of CNC/PVA/CDs composite suspensions. (c) Photograph of CNC/PVA/CDs composite suspensions observed between crossed polarizers.

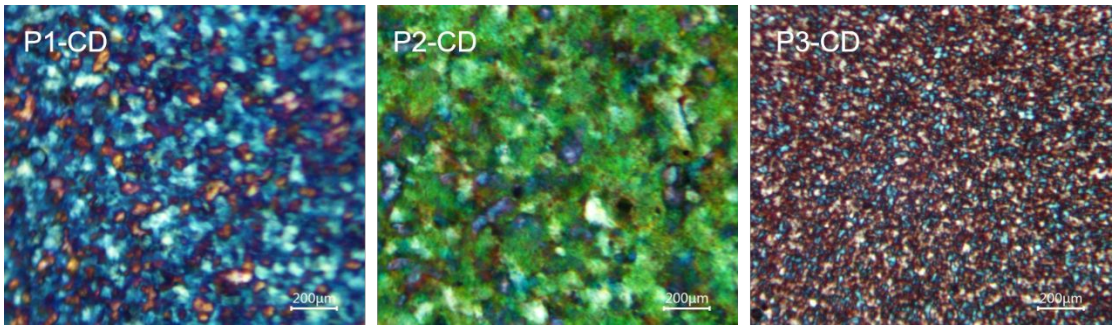

Figure S6. POM images of hybrid photonic films showing tunable birefringent colors.

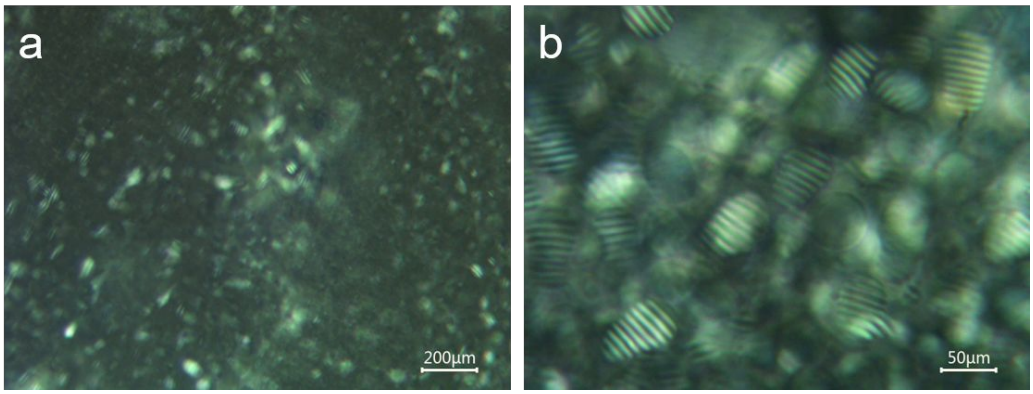

Figure S7. POM images of concentrated CNC/PVA/CDs composite suspension showing the growing tactoids (a) and the coalescing tactoids (b).

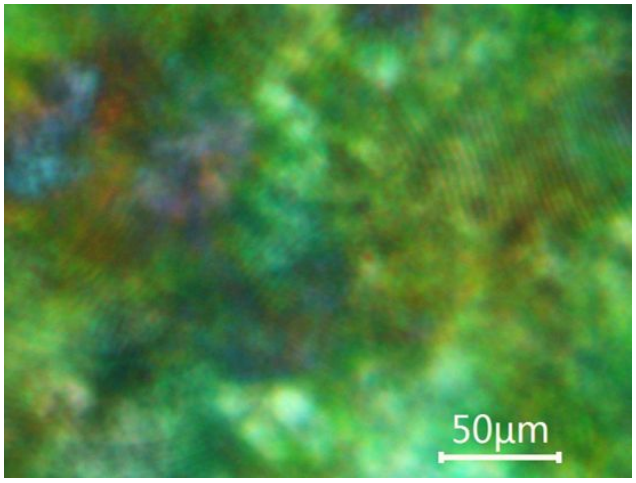

Figure S8. POM image of hybrid chiral photonic film (P2-CD) showing fingerprint defects.

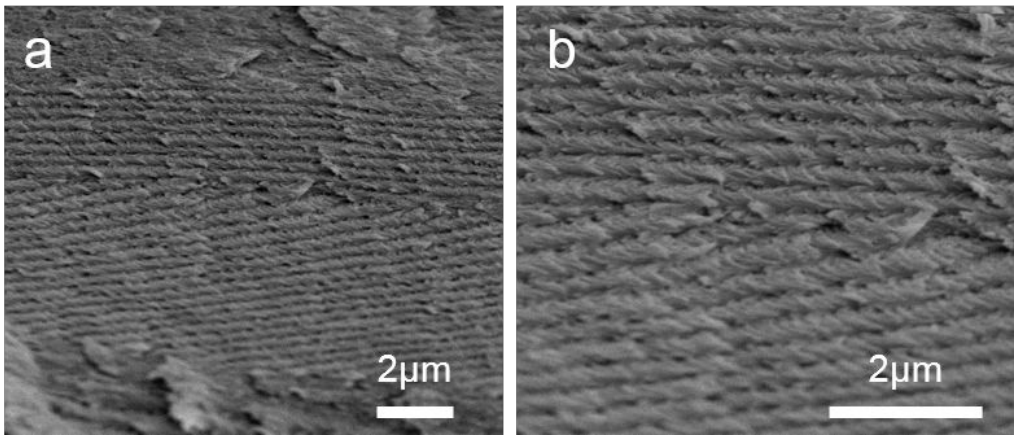

Figure S9. SEM images of hybrid chiral photonic film (P2-CD) showing non-uniform helical axes and varied helical pitches.

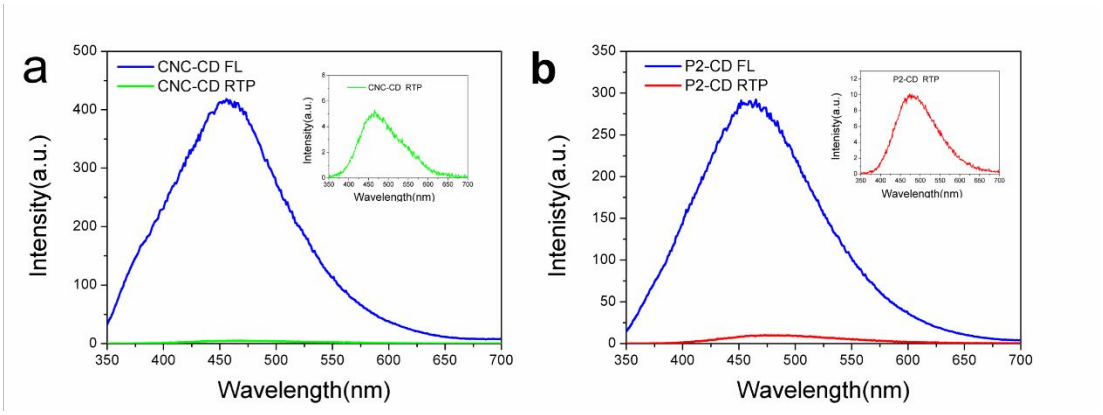

Figure S10. Fluorescence (FL) spectra and room-temperature phosphorescence (RTP) emission spectra of hybrid chiral photonic films for the integral calculation. (a) CNC-CD film; (b) P2-CD film. λ_{ex}=280 nm.

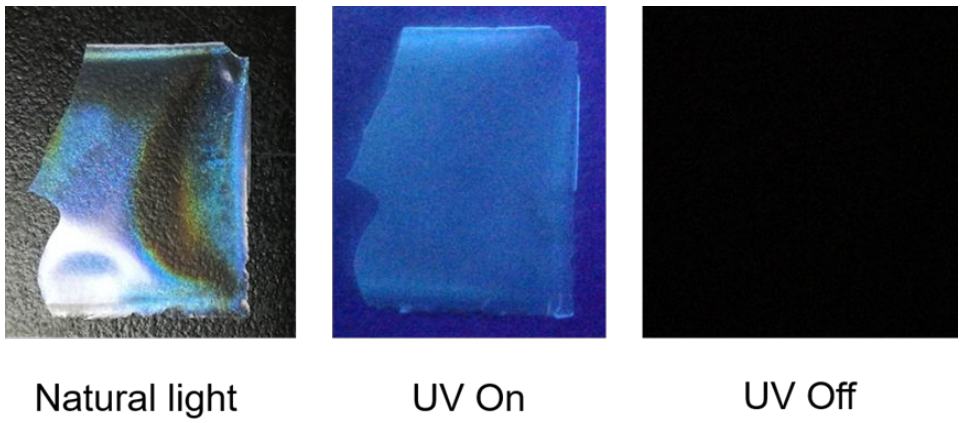

Figure S11. Photograph of CNC-CD film taken under natural light, a 254 nm UV lamp and turning off the UV lamp.

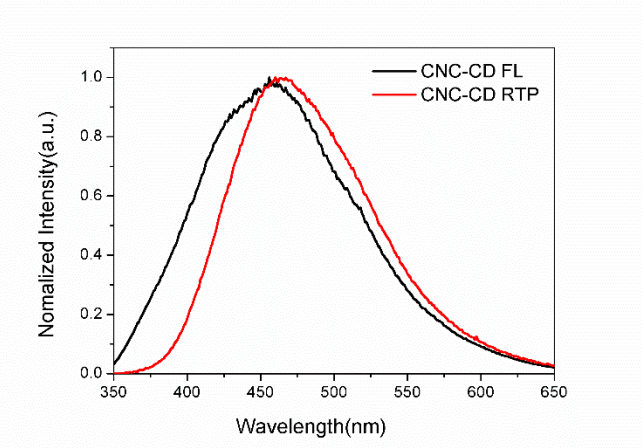

Figure S12. Normalized fluorescence (FL) spectra and room-temperature phosphorescence (RTP) emission spectra of CNC-CD film excited at 260 nm. The delayed time for the measurement of RTP spectra is 0.2 ms.

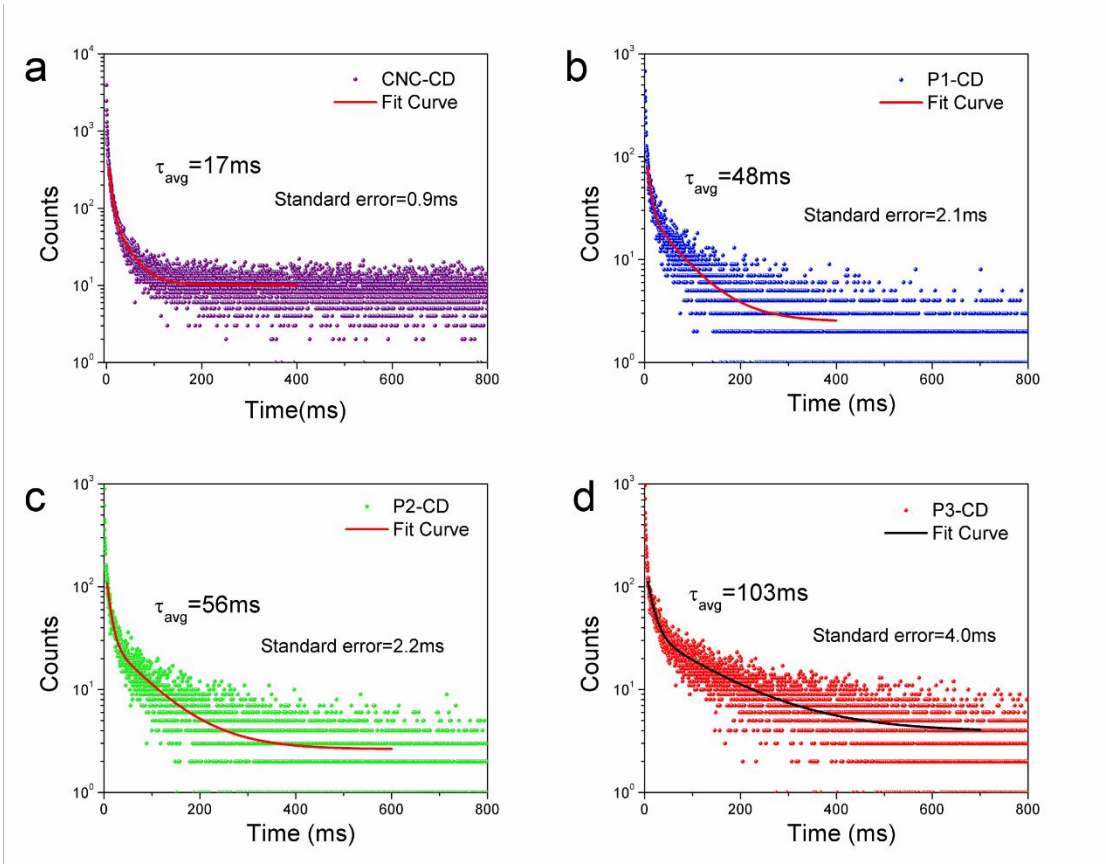

Figure S13. Time-resolved phosphorescence decay curves of hybrid chiral photonic films (λ_{ex}=260 nm, λ_{em}=480 nm).

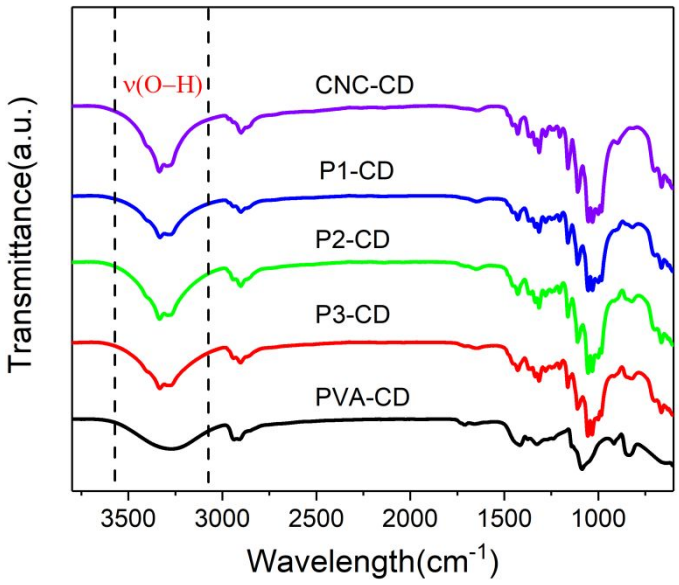

Figure S14. FTIR spectra of hybrid chiral photonic films.

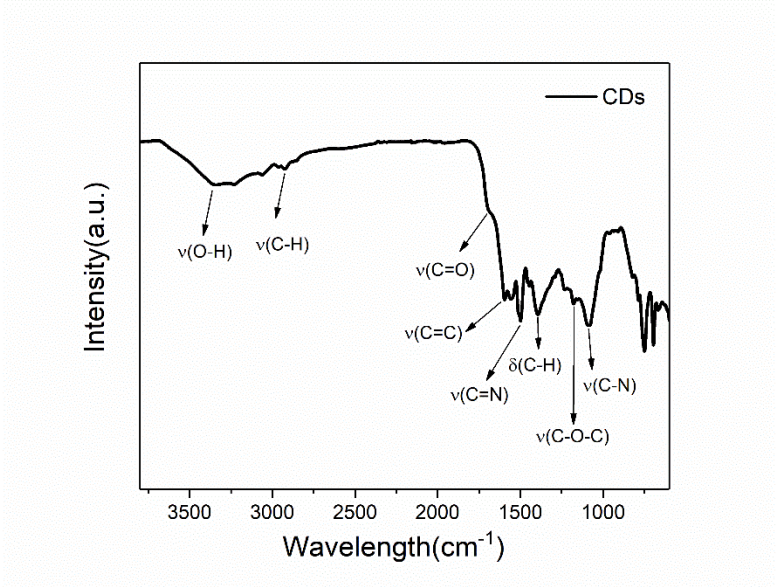

Figure S15. FTIR spectra of CDs.

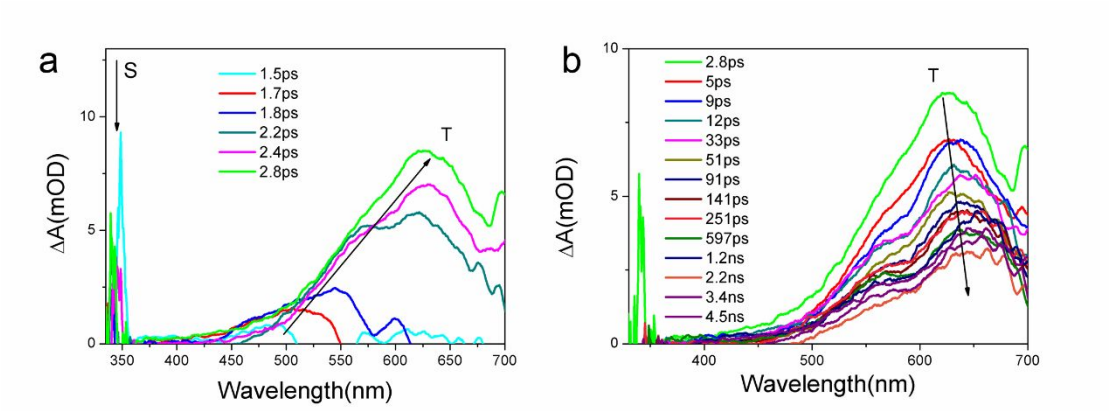

Figure S16. Femtosecond transient absorption (Fs-TA) spectroscopy of CDs solution at different delay times. (a) 1.5-2.8 ps; (b) 2.8 ps-4.5 ns. λ_{ex}=266 nm.

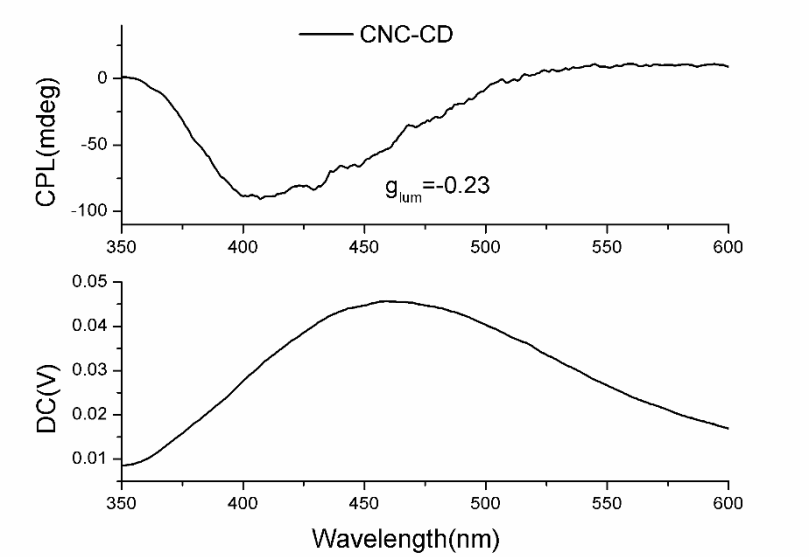

Figure S17. CPL spectra of CNC-CD film.

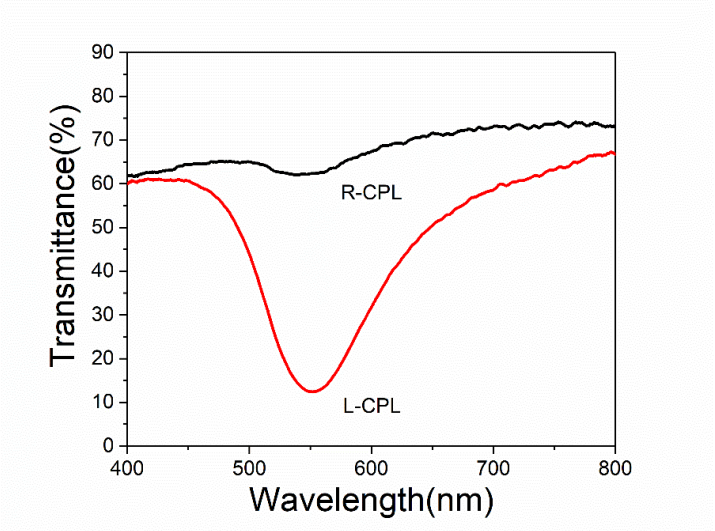

Figure S18. Transmission spectra of P2-CD film probed by L-CPL and R-CPL.

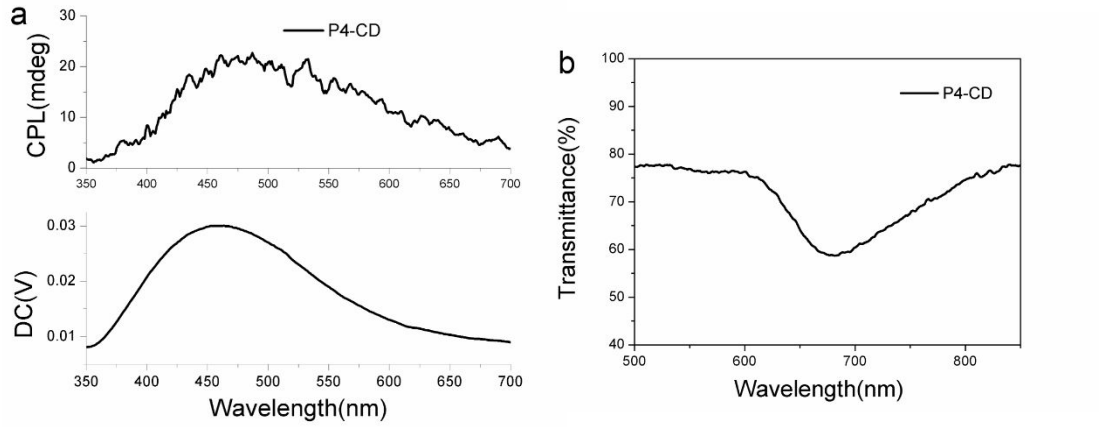

Figure S19. (a) CPL spectra of P4-CD (PBG peak, 680 nm) film. (b) Transmission spectra of P4-CD film.

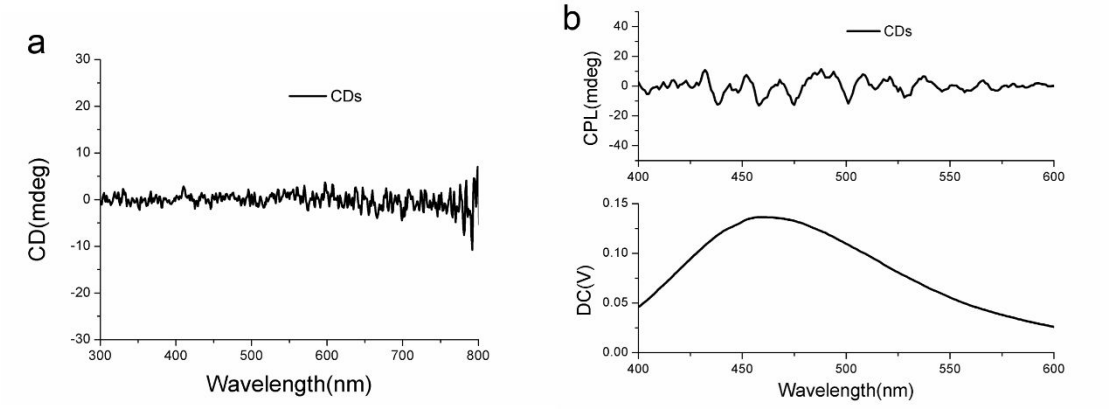

Figure S20. (a) circular dichroism spectra of CDs dispersion. (b) CPL spectra of CDs dispersion.

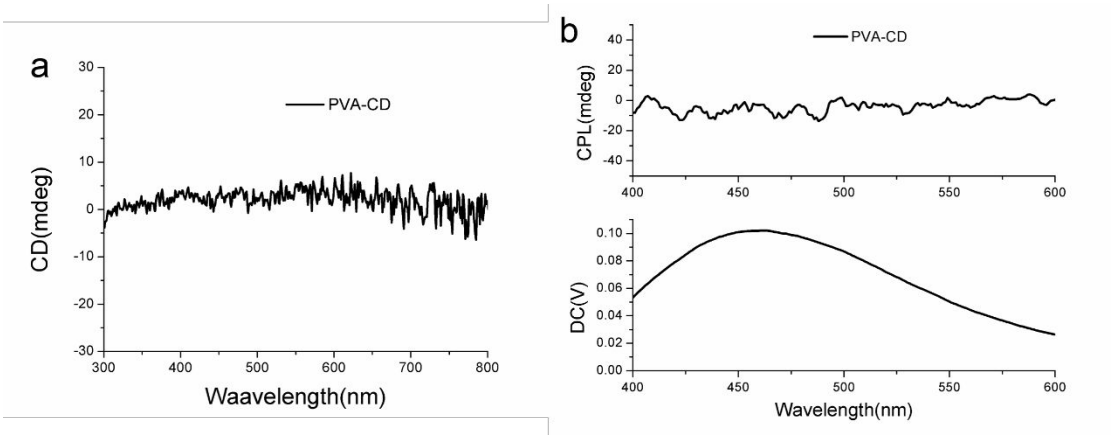

Figure S21. (a) circular dichroism spectra of PVA-CD film. (b) CPL spectra of PVA-CD film.

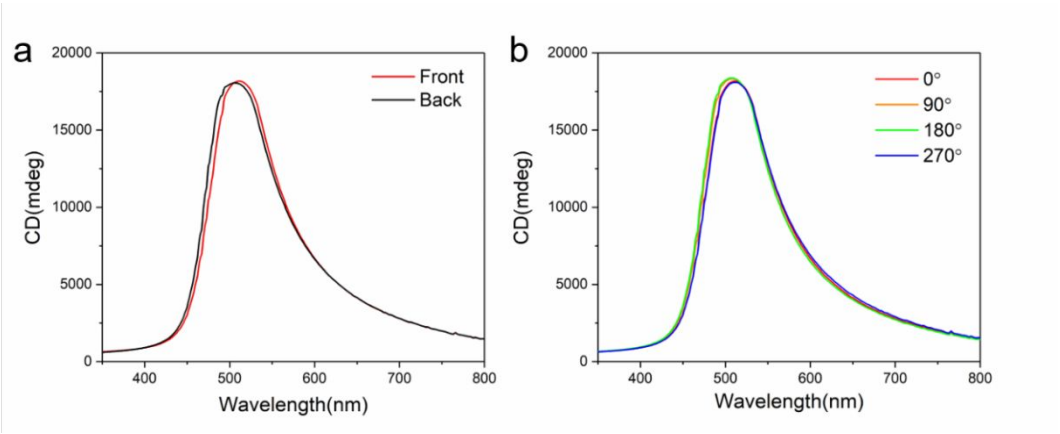

Figure S22. (a) The "front and back" circular dichroism spectra of hybrid chiral photonic film (PVA content, 0.015g); (b) circular dichroism spectra of hybrid chiral photonic film (PVA content, 0.015g) measured at diverse rotation angles.

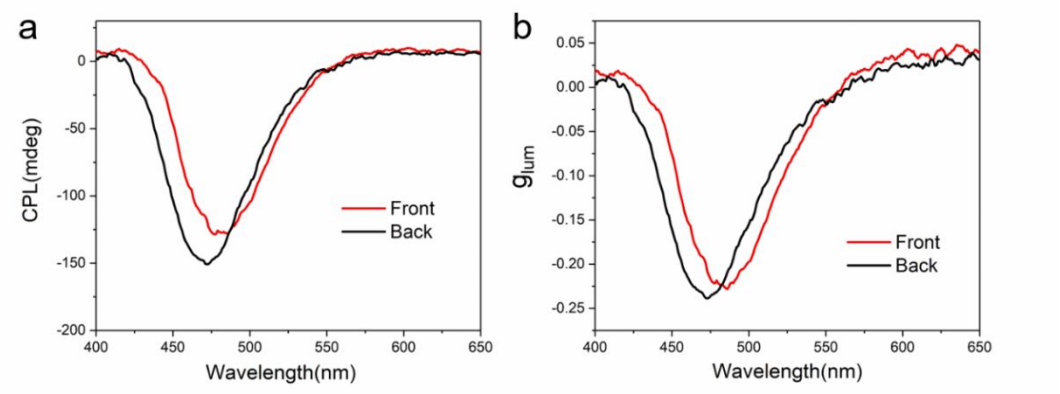

Figure S23. (a) The "front and back" CPL spectra of hybrid chiral photonic film (PVA

content, 0.015g); (b) The "front and back" g_{lum} curve of hybrid chiral photonic film (PVA content, 0.015g).

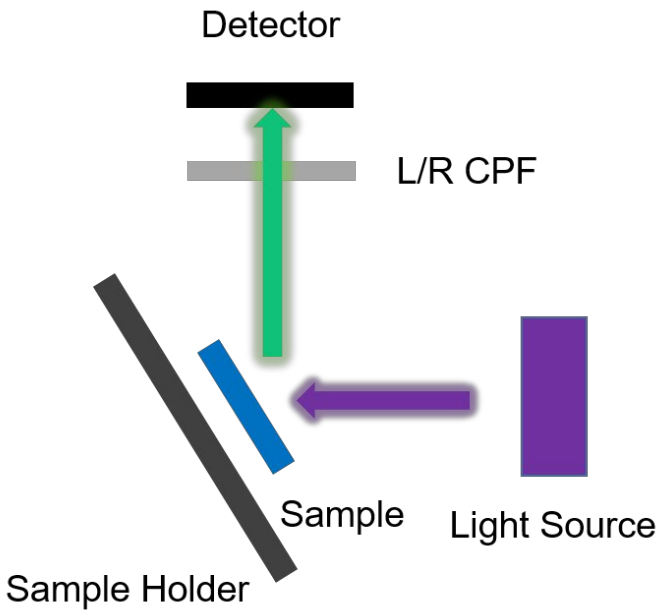

Figure S24. Schematic illustration of the experimental setup for the measurement of CPRTP.

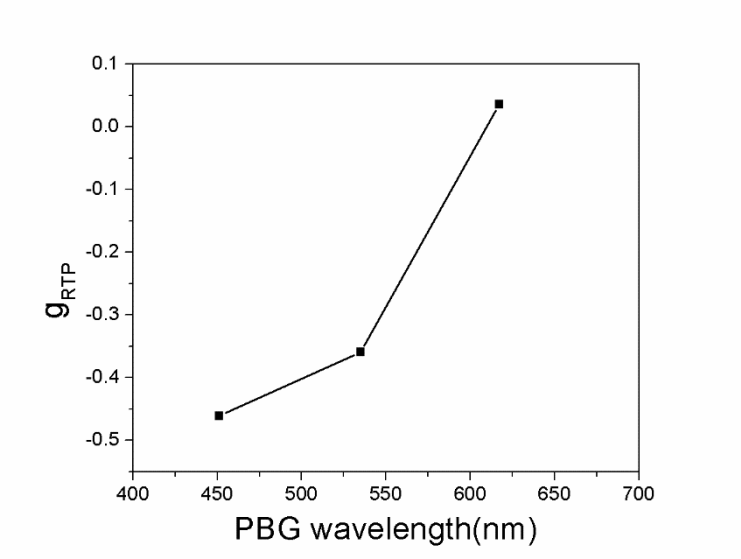

Figure S25. The g_{RTP} curve of hybrid chiral photonic films.

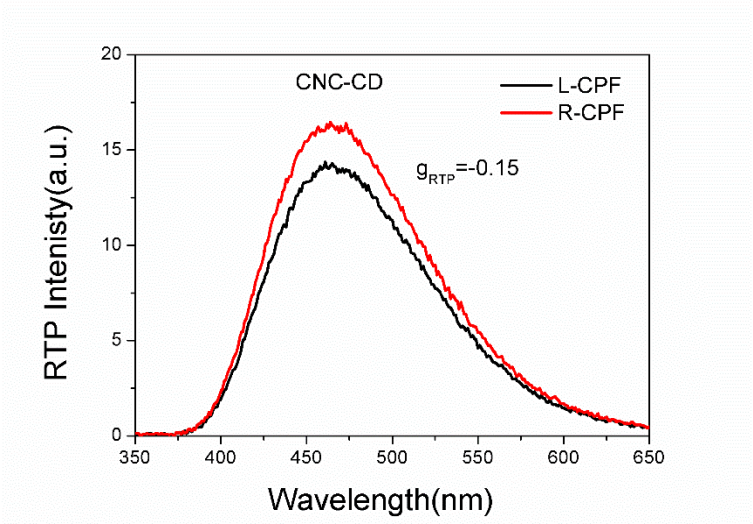

Figure S26. RTP emission spectra of CNC-CD film recorded with an L-CPF or R-CPF.

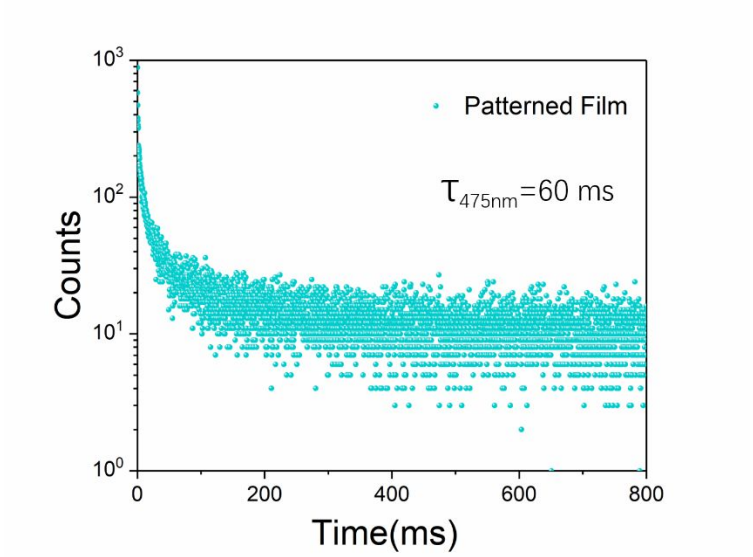

Figure S27. Time-resolved phosphorescence decay curves of patterned photonic film.

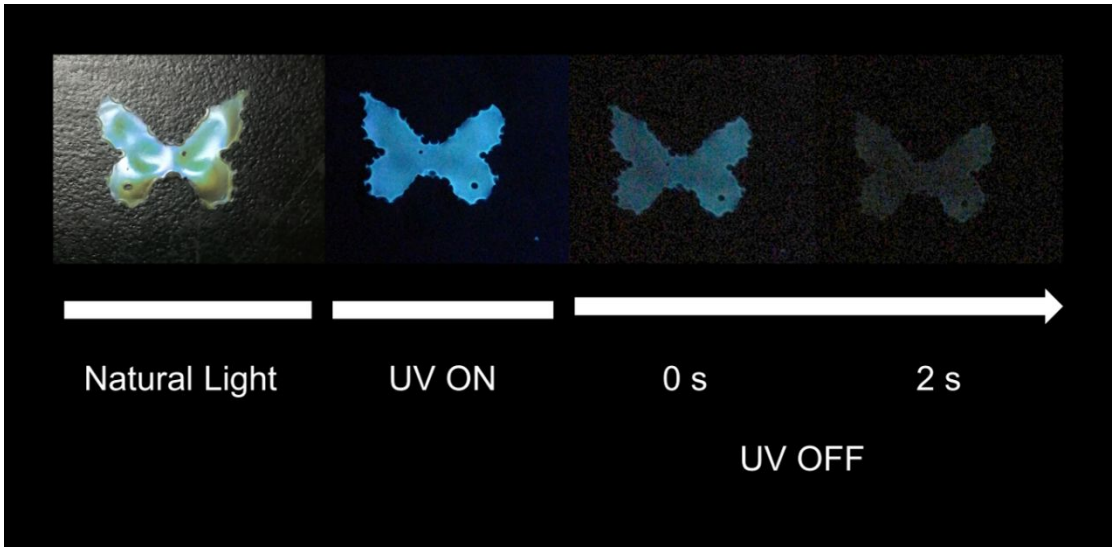

Figure S28. Iridescence and luminescence photographs of a butterfly-patterned film taken under natural light, a 254 nm UV lamp, and at different time intervals after turning off the UV lamp. (from left to right).

Table S1. The dissymmetric factors of circular dichroism spectra for the hybrid photonic films.

Sample	g_{abs}
CNC-CD	0.36
P1-CD	0.29
P2-CD	0.23
P3-CD	0.18

Where g_{abs} is the dissymmetric factor of circular dichroism spectra, and it is calculated according to the following formula:

$$g_{abs} = \frac{ellipticity}{32982 \times Abs}$$

Where Abs is the UV-Vis absorption of the films, and ellipticity (unit: mdeg) is the measured circular dichroism value.

Table S2. Photoluminescence quantum yields and phosphorescence quantum yields of CDs solution and photonic samples. λ_{ex}=280 nm.

Sample	Φ_{PL}	Φ_{phos}
CDs solution	3.6%	–
CNC-CD	2.2%	0.03%
P2-CD	5.2%	0.16%

The phosphorescence quantum yields were calculated as following:

$$\Phi_{phos}=\Phi_{PL}* \frac{A_{RTP}}{A_{FL}+A_{RTP}}$$

Where Φ_{PL} is the absolute total photoluminescence quantum yield, Φ_{phos} is the phosphorescence quantum yield; A_{FL} and A_{RTP} are integral peak areas of fluorescence and phosphorescence (Figure S10 and Table S3).

Table S3. Integral results of the fluorescent spectrum and phosphorescent spectrum for hybrid films.

Sample	A_{FL}	A_{RTP}
CNC-CD	56237	657
P2-CD	40558	1326

Table S4. Phosphorescence lifetime decay parameters of hybrid chiral photonic samples monitored at 480 nm.[a]

Sample	A_1	τ_1 (ms)	A_2	τ_2 (ms)	τ_{avg} (ms)
CNC-CD	607	6	91	31	17
P1-CD	122	7	27	67	48
P2-CD	166	8	29	83	56
P3-CD	124	13	32	136	103

Phosphorescence lifetime calculated following the equation $\tau_{avg} = (A_1\tau_1^2 + A_2\tau_2^2)/(A_1\tau_1 + A_2\tau_2)$, a double exponential function.

Table S5. The standard error of phosphorescence lifetime.

Sample	A_1	τ_1 (ms)	A_2	τ_2 (ms)	τ_{avg} (ms)
CNC-CD	9.9	0.1	4.6	1.1	0.9
P1-CD	6	0.4	1.2	3.2	2.1
P2-CD	4.4	0.2	0.9	2.9	2.2
P3-CD	2.7	0.4	0.9	4.9	4.0

The standard error of phosphorescence lifetime calculated following the equation $\tau_{avg} = (A_1\tau_1^2 + A_2\tau_2^2)/(A_1\tau_1 + A_2\tau_2)$, a double exponential function.

Table S6. the lifetime of carbon dots embedded composite materials.

Material	Life time (ms)	Ref.
CDs@zeolite	22.3	1
CDs@polyurethane	8.7	2
CDs@MnAPO-CJ50	10.9	3
CDs@PVA	380	4
CDs@SiO2	703	5
Pt(II)-Complexe	0.19	6
Chiral organic ionic crystals	862	7
R/S-COOCz	600	8
This study	103	–

REFERENCES

(1) Wang, B.; Mu, Y.; Zhang, H.; Shi, H.; Chen, G.; Yu, Y.; Yang, Z.; Li, J.; Yu, J. Red Room-Temperature Phosphorescence of CDs@Zeolite Composites Triggered by Heteroatoms in Zeolite Frameworks. *ACS Cent. Sci.* **2019,** 5, 349−356.

(2) Tan, J.; Zou, R.; Zhang, J.; Li, W.; Zhang, L.; Yue, D. Large-Scale Synthesis of N-Doped Carbon Quantum Dots and Their Phosphorescence Properties in Polyurethane Matrix. *Nanoscale.* **2016,** 8, 4742−4747.

(3) Wang, B.; Yu, Y.; Zhang, H.; Xuan, Y.; Chen, G.; Ma, W.; Li, J.; Yu J. Carbon Dots in a Matrix: Energy-Transfer-Enhanced Room-Temperature Red Phosphorescence. *Angew. Chem. Int. Ed.* **2019,** 58, 1−7.

(4) Deng, Y.; Zhao, D.; Chen, X.; Wang, F.; Song, H.; Shen, D.; Long Lifetime Pure Organic Phosphorescence Based on Water Soluble Carbon Dots. *Chem. Commun.* **2013,** 49, 5751−5753.

(5) Jiang, K.; Wang, Y.; Cai, C.; Lin, H. Activating Room Temperature Long Afterglow of Carbon Dots *via* Covalent Fixation. *Chem. Mater.* **2017,** 29, 4866−4873.

(6) Schulte, T. R.; Holstein, J. J.; Krause, L.; Michel, R.; Stalke, D.; Sakuda, E.; Umakoshi, K.; Longhi, G.; Abbate, S.; Clever, G. H. Chiral-At-Metal Phosphorescent Square-Planar Pt(II)-Complexes from an Achiral Organometallic Ligand. *J. Am. Chem. Soc.* **2017,** *139,* 6863−6866.

(7) Chen, W; Tian, Z.; Li, Y.; Jiang, Y.; Liu M.; Duan, P. Long Persistent Circularly Polarized Phosphorescence from Chiral Organic Ionic Crystals. *Chem. Eur. J.* **2018,** *24,* 17444−17448.

(8) Li, H.; Li, H.; Wang, W.; Tao, Y.; Wang, S.; Yang, Q.; Jiang, Y.; Zheng, C.; Huang, W.; Chen, R. Stimuli-Responsive Circularly Polarized Organic Ultralong Room Temperature Phosphorescence. *Angew. Chem. Int. Ed.* **2020,** 1−6.